Assessment of Exploitable Geothermal Resources Using Magmatic Heat Transfer Method, Maule Region, Southern Volcanic Zone, Chile

Diego Aravena and Alfredo Lahsen

**Departamento de Geología, Universidad de Chile,
Centro de Excelencia en Geotermia de los Andes (CEGA)**

Keywords

Resource assessment, Maule, Southern Volcanic Zone, volcanic arc, magmatic heat transfer, volcanic system, Monte Carlo, Chile

ABSTRACT

The Andean volcanic arc includes over 200 active stratovolcanoes and at least 12 giant caldera systems. Nevertheless, there is not a standard procedure for estimating geothermal resources associated with unexplored volcanic systems. The study area corresponds to the main cordillera in the Maule region, Chile, along the Southern Volcanic Zone (SVZ) between 34.8º and 36.5º S. The tectonic style and magma emplacement model of this zone favors the occurrence of volcanic associated geothermal systems, due to the presence of shallow magmatic chambers and Cenozoic thrust faults that generate secondary permeability and allows the development of geothermal systems in the upper crust.

In order to identify areas with a high probability of geothermal system development, and using a GIS based superposition method, a geothermal favorability map was created. This favorability map involves using geological, geophysical and geochemical data, which is analyzed in the light of different volcanic related systems around the world.

A GIS-based method is presented for estimating the volume of the volcanic edifice of the major volcanic complexes in the zone. This value is then approximated to the volume of magma emplaced under the volcanoes, and used as a certainty parameter in the magmatic transfer method.

The method of magmatic heat transfer (Smith and Shaw, 1975; Sanyal et al., 2002) was applied in the main volcanic complexes of the area. This method involves using principles of conductive heat transfer and volcanology to calculate temperature distribution in time and space following magma emplacement, then calculates potentially recoverable geothermal energy resources. The analysis of resources obtained for volcanoes in the area includes a variety of factors, such as age, temperature and depth of magma emplacement, and establishes a semi-logarithmic correlation between the resources and the volume of magma emplaced in the upper crust. Other heat-in-place techniques have been developed for estimating geothermal resource size (e.g., Williams et al., 2008; Garg and Combs, 2010; 2011), but these methods are better suited for explored and identified geothermal systems.

The mean calculated resources for the Maule region are ~1,400 MWe. These values are distributed between five main eruptive complexes with individual values that range from 177 to 392 MWe for 30 years.

1. Introduction

The Andean volcanic arc includes over 200 potentially active Quaternary volcanoes, and at least 12 giant caldera/ignimbrite systems, occurring in four separate segments referred to as the Northern (ZVN; 2ºN-5ºS), Central (ZVC; 14-28ºS), Southern (ZVS; 33-46ºS) and Austral (ZVA; 49-55ºS) Volcanic Zones. Volcanism results from subduction of the Nazca and Antarctic oceanic plates below South America (Stern, 2004).

Geothermal exploration in Chile is currently very active and is driven by the need for energy security and stability. The country presents more than 300 geothermal areas located along the Chilean Andes and associated with Quaternary volcanism. The main geothermal areas take place in the extreme north (17°-28°S) and central-southern part (33°-46°S). In areas where the Quaternary volcanism is absent, such as along the volcanic gaps of Andean Cordillera (28°-33° and 46°-48°S), as well as in the Coastal Range, thermal springs are scarce and their temperatures are usually lower than 30°C (Lahsen et al., 2010).

Preliminary assessment of the geothermal potential of the north and central-southern volcanic-geothermal zones gives a value in the order of 16,000 MW for at least 50 years from the geothermal fluids with temperatures exceeding 150°C, and located at a depth less than 3,000 m (Lahsen, 1986). Nevertheless, there is not a standard procedure for estimating geothermal resources associated with unexplored volcanic systems and, presently, the Andean volcanic arc represents one the largest undeveloped geothermal provinces of the world.

2. Geologic and Tectonic Framework

The area investigated (Fig. 1) lies on the crest and western slope of the Andes at about 34.8º to 36.5º S in the Maule (VII) region. Central Chile is here only 170 to 210 Km wide and morphologically divided into a Coastal Cordillera, Central Valley, and Andean Cordillera.

Between 33ºS and 36ºS, the belt of active stratovolcanoes lies ~260 Km east of the axis of the Chile trench and ~90 Km above the top of a Wadati-Benioff zone that dips ~20ºE (Hildreth et al., 1984). Regional-scale rock units are organized into several margin–parallel belts, ranging from Paleozoic plutonic and metamorphic rocks in the Coastal range to Meso–Cenozoic plutonic and volcano-sedimentary units in the Main cordillera. The Central Depression, located in the middle, is characterized by Oligocene to recent volcano-sedimentary rocks. The basement of the volcanic arc between 33° and 37°S is made up of extensive outcrops of Meso–Cenozoic volcano–sedimentary rocks, only locally intruded by Mio–Pliocene plutons (Charrier et al., 2002).

Pliocene and Quaternary rocks of this part of the Andes are essentially undeformed but include complex intracanyon assemblages, chiefly of andesitic to dacitic lavas, tuffs and agglutinates that erupted for the most part from long-lived composite centers (Hildreth et al., 1984). The main volcanic complexes in the area, and their morphology, can be observed in Fig.5.

In Central Chile, between 33°S and 34°30′S, volcanism is coeval with current east–west compression. Magmas feeding stratovolcanoes are proposed to ascend through a composite system of subhorizontal reservoirs and ancient/active thrusts (Fig. 2). Volcanoes between 34°30′S and 36°S sit on top of ancient reverse faults and/or WNW-striking basement faults that may connect downwards with tension cracks associated with a concealed dextral strike–slip fault zone (Fig. 2).

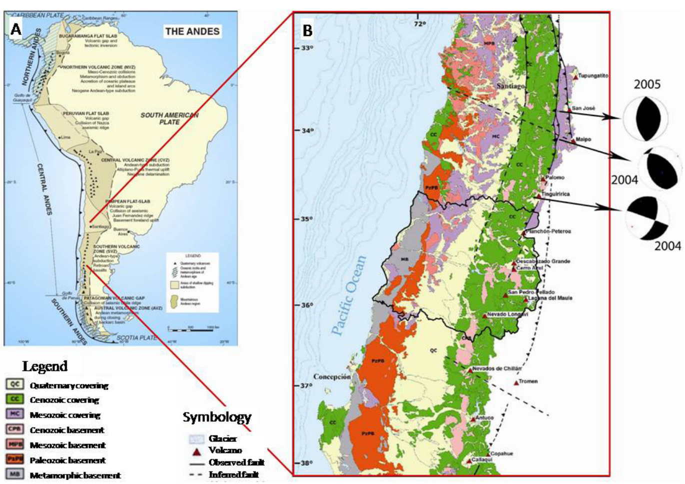

Figure 1. (A) Major segments of the Andes and their main quaternary volcanic zones. (B) Regional geological map between 33º and 38º S, Maule region outlined in black. Modified from Cembrano and Lara (2009).

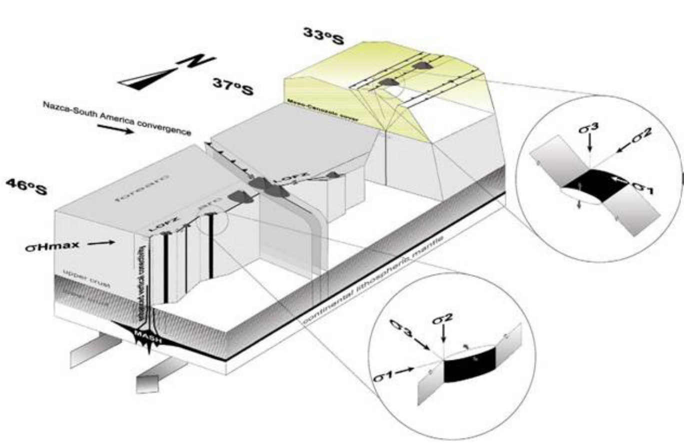

Figure 2. Cartoon that summarizes the first- and second-order factors that control volcano–tectonic associations in the Southern Andes Volcanic Zone (not to scale; Cembrano and Lara, 2009).

3. Favorability Model

The favorability model method involves using geological, geophysical, and geochemical data to identify areas that are likely to present geothermal potential. Favorable and unfavorable geothermal terrains were defined using a weighted overlay superposition model and a multi-class favorability ranking (Table 1), presenting six separate layers of evidence; young volcanic rocks, proximity to eruptive centers, young fault density, proximity to geothermal prospects and hot springs, remotely sensed geothermal-related minerals and upper crust earthquake density.

These six evidence layers were chosen because they can be easily shaped into evidence maps in raster format and they can be obtained from publically available sources. Several works support the association of the evidence layers with the presence of geothermal systems (e.g., Koenig and McNitt, 1983; Hanano, 2000; Blewitt et al., 2003; Julian and Foulger, 2004; Coolbaugh et al., 2007; Noorollahi et al., 2007; Kratt et al., 2010). These studies were used to assign a set of suitability and weighting factors for each layer (Table 1).

The favorability model was developed using the raster calculator tool within Arc Map. This tool reclassifies the pixel values in

Table 1. Multi-class favorability ranking for the six separate layers of evidence. Hydrothermal minerals are present in most of the volcanic zone; therefore a higher weight is not assigned to this layer.

Data	%	Layer	%	Class	Value
Geological	60	Volcanic rocks	40	Absent	1
				Mixed	5
				Present	9
		Fault density (m/Km2)	20	< 35	1
				35 - 100	5
				> 100	9
		Proximity to Volcano (Km)	40	> 15	1
				7 - 15	5
				< 7	9
Geochemical	30	Proximity to hot springs (Km)	40	> 10	1
				5 - 10	5
				< 5	9
		hydrothermal mineral occurrence	60	Low	3
				High	9
Geophysical	10	Earthquake density (Eq./Km2)	100	< 0,002	1
				0,002 - 0,02	5
				> 0,02	9

the input rasters onto a common evaluation scale of suitability. Then each input raster is weighted according to its importance and added to produce the output raster. The weight is expressed as a relative percentage, and the sum of the percent influence weights must be equal to 100% (Noorollahi et al., 2007). Finally, we classified the study area into different levels of favorability based on exploration data (Fig. 3.).

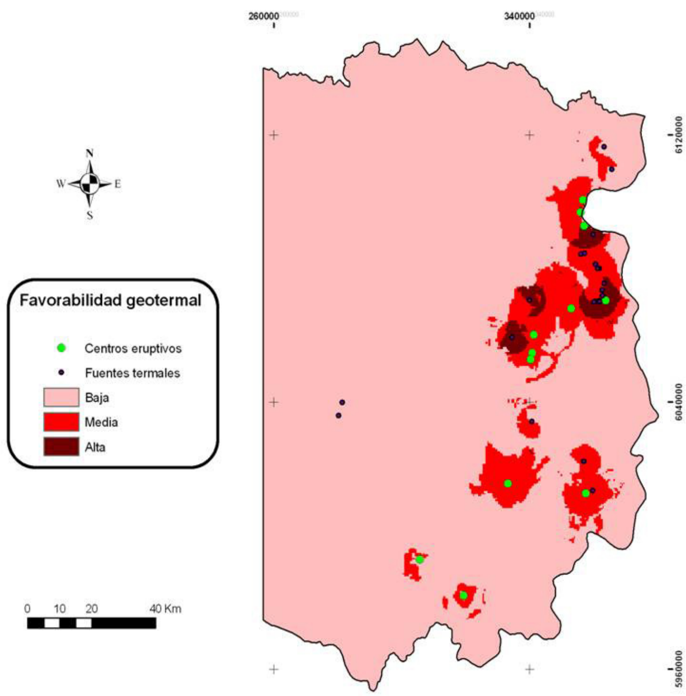

Figure 3. Final map of geothermal favorability for the Maule Region.

4. Resource Assessment

In a volcanic geothermal system the ultimate heat source is the magma emplaced at relatively shallow levels beneath the ground surface as part of the process of volcanic activity.

For this work, we used the solution for a cooling magma body as described in Sanyal et al. (2002). Using principles of conductive heat transfer and volcanology, we can approximate the temperature at any depth under a surface location, at any distance from the magma chamber, at any time after magma emplacement. Then, it is possible to calculate potentially recoverable geothermal energy resources associated with a single volcano or volcanic complex. Conductive heat transfer from a magma body to the surrounding rock can be calculated if one can estimate the following basic parameters of the magma: volume, depth of burial, age and initial temperature (Sanyal et al., 2002).

The fixed and uncertain parameters used in the estimate for the Maule region can be observed in Tables 2 and 3. They were selected based on the geodynamic context that characterizes the Andean volcanism and some values are extracted from previous works involving specific studies for each volcano in the area (e.g., Lopez and Munizaga, 1983; Hildreth et al., 1984; Grunder and Mahood, 1988; Grunder et al., 1987; Naranjo and Haller, 2002; Sellés et al., 2004).

Table 2. Fixed parameters for magmatic heat transfer calculations.

Fixed Parameter	Value	
Initial vertical temperature gradient	45	ºC/Km
Maximum Depth considered for estimation	4	Km
Density of rock	2700	Kg/m3
Thermal diffusivity	0.025	KJ/m/s/ºC
Porosity of rock	3	%
Rejection temperature	14	ºC
Cut-off resource temperature	200	ºC
Specific heat of rock	1	KJ/Kg/ºC
Specific heat of fluid	2.08	KJ/Kg/ºC
Power plant life	30	years
Utilization factor	0.45	
Power plant capacity factor	0.8	
Recovery factor	0.05	

Table 3. Uncertain parameters with their respective maximum and minimum used in calculations.

Volcanic Complex	Age (Ky)		Emplacement Temperature (ºC)		Emplacement Depth (Km)	
	Min	Max	Min	Max	Min	Max
Planchon-Peteroa-Azufre	350	550	1000	1100	3	7
Complejo Caldera Calabozos	120	350	800	1000	3	7
Descabezado grande - Quizapu - Cerro Azul	120	350	817	870	4	7
San Pedro - Tatara - Laguna del Maule	120	350	900	1200	3	7
Nevado de Longavi - Lomas Blancas	120	350	900	1200	3	7

Finally, for the calculation process, we assigned a depth and horizontal distance of 4 and 7 km respectively. These values corresponds to a relatively easy to drill depth and a horizontal distance of rock temperatures over 200 ºC (Cut-off resource temperature) as seen in Figure 4.

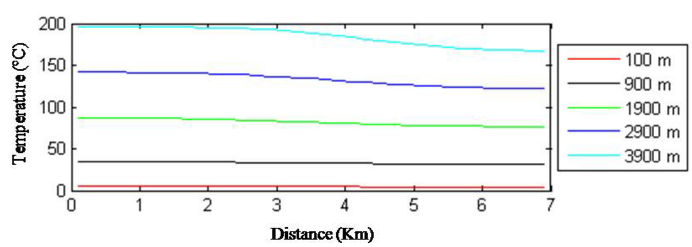

Figure 4. T distribution around a 10 km^3 magmatic body, at a depth between 3 and 7 (km) and emplaced 120 to 550 kyears ago with an initial temperature between 800 and 1200 °C. These results are based on a conductive heat model and convection might result in lower temperatures over time; in order to reduce this effect we used an increased value for the thermal diffusivity (Table 2).

4.1. Volume Estimation

Typically, the amount of material extruded as lava or pyroclastic material is balanced by a similar amount of magma located in shallow areas of the upper crust (Sanyal et al., 2002). Therefore, the volume of the magmatic complex located beneath the volcano can be roughly estimated by determining the volume of extruded material. This approximation may underestimate the heat source size, as Crisp (1984) suggests that the ratio of intrusive to eruptive volumes for silicic volcanic centers in the Andes is ~6:1.

For many volcanoes, most of the extruded material may be stored as part of the volcano today. This is particularly true for conical geometry stratovolcanoes of the Maule region, where the eruptive activity is dominated by lava flows and moderately explosive pyroclastic eruptions. In these cases, the volume of the volcano represents a good estimate of the minimum volume of the igneous complex that is available to act as a geothermal heat source.

In this paper, we propose an alternative methodology for calculating the geometric volume of the volcanic edifice, involving the use of geographic information systems (GIS). Volume variations due to a larger eruptive history are not taken into account since this is a first order approximation and the time window used for each volcanic complex is relatively small (~200 Ka). This estimate is considered more robust and considers the volume as a fixed parameter (instead of an uncertainty parameter) in the Monte Carlo simulation.

To estimate the volume of each volcanic complex, we use the tool *Surface volume* from the *3D analyst* extension in ArcGIS. From a digital elevation model (DEM) and estimating a horizontal plane (baseline) as the base of the complex, this software provides the volume between the horizontal plane and the topography determined by the DEM. Estimating the proper plane, from which the volume is measured for each edifice, is performed by analyzing the geometry of the volcano, selecting areas with greater variation in the slope with the topographic profiles (Fig.5). This method is inherently accompanied by the risk of overestimation when the volcanic edifice is built on an inclined basal plane, so special care must be taken into account for each individual edifice. Finally, the volume of the magma chamber is estimated using a 1:1 ratio respecting the calculated volume for each volcanic edifice.

For this work, we have used the solution for a cubic chamber and an instantaneous source, as described in Sanyal et al. (2002). Therefore the assumed diameter of the magma body corresponds to the cube root of the chamber volume.

This method presents several sources of error that have to be considered, but ambiguities in defining the edifices spatially are by far the largest source of uncertainty. Although this work doesn't have an error analysis for this method, we recommend a careful field study for each volcanic complex in order to understand the sensitivity of the estimation to uncertainties of the baseline.

4.2. Monte Carlo Simulation

The Monte Carlo simulation is a quantitative technique that uses statistics and computers to imitate, using mathematical models, the random behavior of real systems. Usually when it comes to systems whose state changes over time, we use discrete event simulation (Faulín and Angel, 2005). This technique combines statistical concepts (random sampling) with the ability of computers to generate pseudo-random numbers and automate calculations.

In this paper we implemented the Monte Carlo method using MATLAB 7.0.1. This program is used both to simulate the tem-

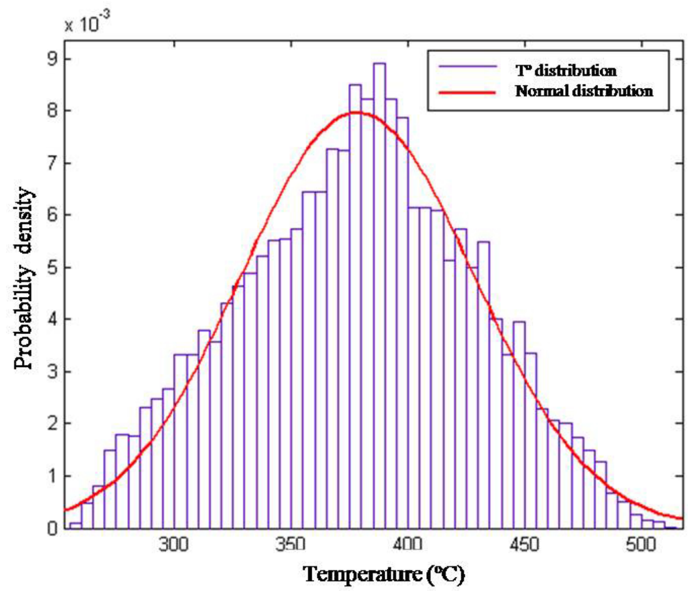

Figure 6. T probability distribution around the Planchón-Peteroa associated magmatic body. T obtained at 4 km depth, located directly on the eruptive center (x=0).

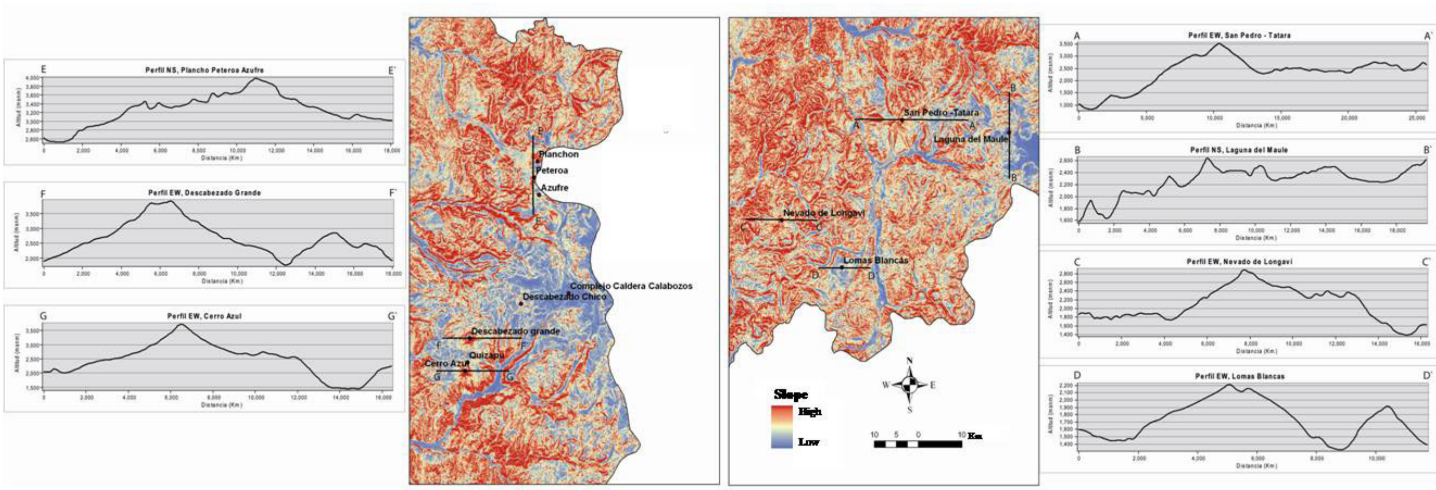

Figure 5. Slope map and topographic profiles of the main volcanoes in the studied area.

perature distribution around a magmatic body and to compute the geothermal resources associated with this temperature distribution. The use of this simulation is considered necessary since there are three parameters of uncertainty in performing the estimate: depth, temperature and age of magma emplacement.

Fig. 6 shows a histogram, after 10,000 iterations, with the temperature probability distribution at 4 Km. of depth and directly over the eruptive center (x=0), for the Planchón-Peteroa volcanic complex. The red curve is a fit of the results by adjusting to a normal distribution. This approach will allow obtaining the temperature distribution around the magmatic body with a probability of 90%.

4.3. Results

Fig. 7 shows the temperature distribution around the Planchón-Peteroa volcanic complex. Temperature curves vary depending on the horizontal distance and depth for each eruptive center (with a 90% probability).

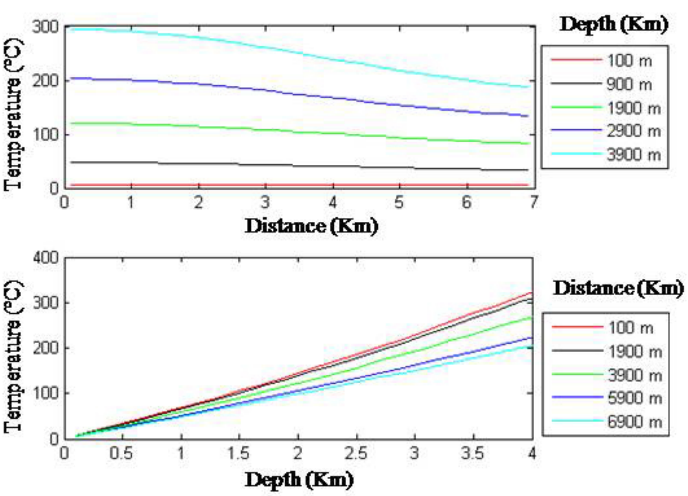

Figure 7. Temperature distribution graph for the Planchón-Peteroa volcanic complex. Curves are based on the distance from the margins of the magma body.

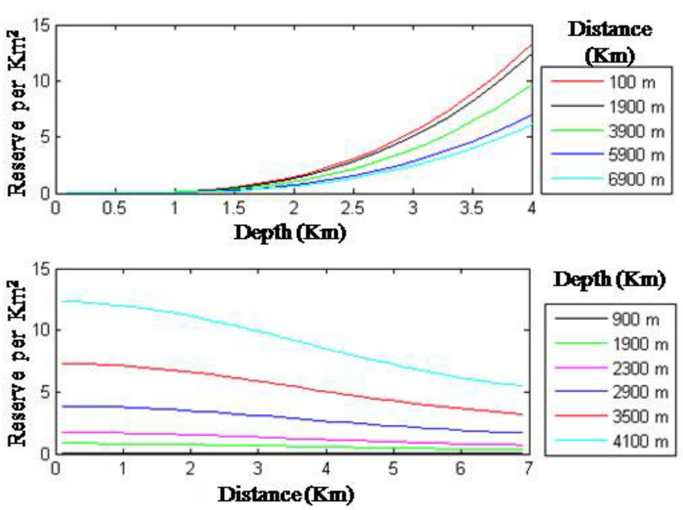

Figure 8. Geothermal resources distribution graph for the Planchón-Peteroa volcanic complex. Curves are based on the distance from the margins of the magma body.

Fig. 8 shows the geothermal resource distribution for the Planchón-Peteroa volcanic complex. The curves represent geothermal resources per square kilometer as a function of horizontal distance and depth.

Table 4 shows the estimated volume as well as the mean calculated resources for each volcanic complex. The total estimated geothermal resources for the Maule region are ~1,400 MWe.

5. Discussion

5.1. Favorability Map

Fig. 3 shows the final map of geothermal favorability obtained from the weighted overlay. As expected, there is a clear correlation with eruptive centers, showing areas of high geothermal favorability on the north and west slopes of the Descabezado Grande volcano, in the central area of the Calabozos Caldera complex and on the south-southeast slopes of the Azufre volcano. Areas of medium favorability are observed all around the Planchón-Peteroa, Calabozos Caldera and Descabezado Grande-Quizapu-Cerro Azul complexes.

Volcanoes located further south (Lomas Blancas, San Pedro-Tatara, Laguna del Maule and Longaví) show only areas of medium favorability. This is mainly associated with the low number of hot springs that have been explored in this area, and it is considered that a more detailed sampling of these sectors could increase the degree of favorability associated with these complexes.

5.2. Volume-Resource Relation

Fig. 9 shows geothermal resource curves as a function of emplaced magma volume. For these estimates we assume a normal initial temperature of magma between 1000 and 1200 °C. As discussed below, the initial temperature can affect these results, so special care must be taken into account when analyzing magmas with different properties. We compare curves for a body emplaced at 3 to 5 (full lines) and 5 to 7 km (dashed lines). The ages of emplacement vary from 120 to 350 (red lines) and 350 to 550 (Ky) (blue lines).

Estimated geothermal resources show a logarithmic behavior with respect to the volume of magma emplaced. From this, it follows that there are ranges of volume where the resource varies considerably as the amount of emplaced magma changes. This is especially true for volumes under 500 km^3, where a strong dependence between resources and volume can be observed. On the other hand, if large volumes are used (>500 Km^3), it does not imply a proportional increase in resources associated with the eruptive center. Also, when analyzing the resource curves for a body located between 3 and 5 km depth (solid curves), there is a crossing for a ~22 km^3 body. This is an indicative of the volume limit at which resources are greater for younger or older volcanoes due to the reaching of a post-magmatic stage. Nevertheless, this volume limit must be carefully analyzed, since this value will shift greatly as we vary any other parameter.

Fig. 4 shows a graph of temperature distribution around a magmatic body of 10 km^3, with age and depth varying from 120 to 550 (Ky) and 3 to 7 (Km), respectively. The initial temperature of magma is uniformly distributed between 800 and 1200 °C. This graph shows how the temperature curves never exceed 200 °C, so

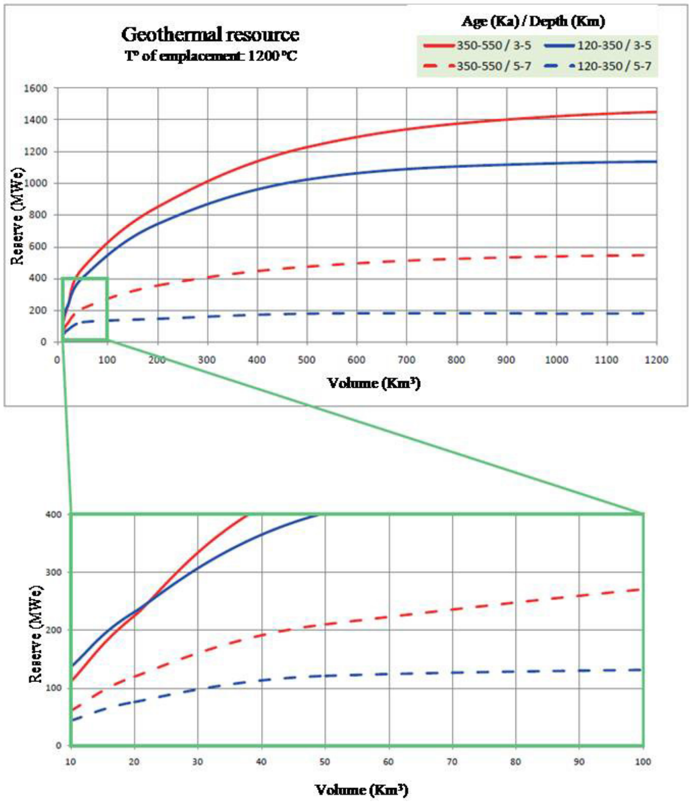

Figure 9. Geothermal resource versus volume for a magmatic body with initial temperature between 1000 and 1200 °C. Compared curves for bodies emplaced to a depth of 3 to 5 and 5 to 7 (km), with ages varying from 120 to 350 and 350 to 550 (ky).

that the rock temperature does not exceed the cut-off temperature imposed for electricity generation. Therefore, it is possible, just by using graphs of temperature distribution, to determine a lower volume limit for which a magmatic body is capable of providing sufficient heat needed for electrical generation.

The notion that the volume-age relationship determines the possible geothermal potential is consistent with the analysis of Smith and Shaw (1975), whereby an igneous system can reach a post-magmatic stage of cooling, which is achieved earlier for small volumes (hence the curves cross in Fig. 9.

Table 4. Volume and mean resources estimated for each volcanic complex in the study area. The volume of lava extruded by the Calabozos Caldera Complex is not determined by this method, due to the wide expanse of the Loma Seca Formation, which is largely covered by Quaternary volcanism. Therefore, we used the previously estimated value from Hildreth et al. (1984).

Volcanic Complex	Volcanic Edifice Volume (Km^3)	Mean Reserve (MWe)
Planchon-Peteroa-Azufre	43.2	233
Complejo Caldera Calabozos	1050.0	392
Descabezado grande - Quizapu - Cerro Azul	102.7	177
San Pedro - Tatara - Laguna del Maule	415.8	346
Nevado de Longavi - Lomas Blancas	148.8	248

5.3. Estimation Parameters

A sensitivity test shows that the depth of emplacement of the magma is, by far, the uncertainty parameter that most influences the resource estimation, generating variations of up to 70%. This variation is clearly observed in Fig. 9, when comparing the curves of the same color (solid versus dotted line).

The age of emplacement is a factor which, although less influential than the depth, has an important influence with results varying up to 30% (red versus blue line in Fig. 9). Age and depth related variations are enhanced as the volume of magma increases.

The initial temperature of the magma is the uncertainty parameter that has less influence on the results, producing variations of up to 10%, which, despite being small compared with the other factors, has an influence that must be taken into account.

6. Conclusions

Through the analysis of geological, geochemical and geophysical evidence, and using the weighted overlay superposition method, it was possible to generate a map of geothermal favorability in the study area.

The methodology for estimating volume of volcanic edifices by geographic information systems (GIS) is presented as an objective tool to estimate the minimum volume of magma emplaced under a volcanic complex. The 3D analyst extension of ArcMap 9.3 allows for an estimation of the volume of regional lavas, using as input a 1:1,000,000 scale map and a digital elevation model (DEM).

Based on available geological data, and using the magmatic heat transfer method, we calculated the exploitable geothermal resources associated with volcanic systems in the Maule region. This assessment is based on inferred resource estimations and yields values of ~1,400 MWe, which are distributed between five major eruptive complexes (Table 4).

It was possible to characterize the magmatic heat methods sensitivity with each of the uncertainty parameters and its correlation with the volume of magma emplaced. It is considered that there is an upper limit of magma emplaced, from which recoverable resources have very slight variations as the magma emplaced increases. In turn, there is a lower volume from which resources are not high enough for electricity generation and, in some cases, it is possible to determine the age-volume relation in which greater resources are expected. There is significant reliance on other parameters like depth of emplacement, initial temperature of magma and recovery factor.

A sensitivity analysis of the magmatic heat method, yielded changes in the resources of: i) up to 70% depending on the depth of emplacement of the magma, ii) up to 30% depending on the age of emplacement and iii) up to 10% depending on the initial temperature of the magma.

7. References

Blewitt, G., Coolbaugh, M., Holt, W.E., Kreemer, C., Davis, J.L., and Bennett, R.A. (2003). Targeting potential geothermal resources in the Great Basin from regional- to basin-scale relationships between geodetic strain and geological structures. *Geothermal Resources Council Transactions 27*, 523-527.

Cembrano, J., and Lara, L. (2009). The link between volcanism and tectonics in the southern volcanic zone of the Chilean Andes: A review. *Tectonophysics* 471, 96-113.

Charrier, R., Baezar, O., Elgueta, S., Flynn, J.J., Gans, P., Kay, S.M., Muñoz, N., Wyss, A.R., and Zurita, E. (2002). Evidence for Cenozoic extensional basin development and tectonic inversion south of the flat-slab segment, southern Central Andes, Chile (33º-36º S.L.). *Journal of South American Earth Sciences* 15, 117-139.

Coolbaugh, M.F., Kratt, C., Fallacaro, A., Calvin, W.M., and Taranik, J.V. (2007). Detection of geothermal anomalies using Advanced Spaceborne Thermal Emission and Reflection Radiometer (ASTER) thermal infrared images at Bradys Hot Springs, Nevada, USA. *Remote Sensing of Environment 106*, 350–359.

Crisp, J.A. (1984) Rates of magma emplacement and volcanic output. *Journal of Volcanology and Geothermal Research 20*, 177-211.

Faulín, J., & Ángel, J.A. (2005). *SIMULACIÓN DE MONTE CARLO CON EXCEL.* Secretaría de Estado de Educación y Universidades (MECD).

Garg, S. K., and Combs, J. (2010). Appropriate Use Of Usgs Volumetric "Heat In Place" Method And Monte Carlo Calculations. *PROCEEDINGS, Thirty-Fourth Workshop on Geothermal Reservoir Engineering.* Stanford University, Stanford, California.: SGP-TR-188.

Garg, S., and Combs, J. (2011). A Reexamination Of USGS Volumetric "Heat In Place" Method. *PROCEEDINGS, Thirty-Sixth Workshop on Geothermal Reservoir Engineering.* Stanford University, Stanford, California.: SGP-TR-191.

Grunder, A.L., and Mahood, G. A. (1988). Physical and Chemical Models of Zoned Silicic Magmas: The Loma Seca Tuff and Calabozos Caldera. *Journal of Petrology* , 831-867.

Grunder, A.L., Thompson, M.J., and Hildreth, W. (1987). The Hydrothermal System of the Calabozos Caldera, Central Chilean Andes. *Journal of Volcanology and Geothermal Research* 32, 287-298.

Hanano, M. (2000). Two Different Roles of Fractures in Geothermal Development. *Proceedings World Geothermal Congress*. Kyushu - Tohoku, Japan.

Hildreth, W., Grunder, A.L., and Drake, R.E. (1984). The Loma Seca Tuff and the Cabalozos caldera: A major ash-flow and caldera complex in the southern Andes of central Chile. *Geological Society of American Bulletin* 95, 45-54.

Julian, B.R., and Foulger, G.R. (2004). Microearthquake Focal Mechanisms: A Tool for Monitoring Geothermal Systems. *Geothermal Resources Council Bulletin 33*, 166-171.

Koenig, J.B., and McNitt, J.R. (1983). Controls on the location and intensity of magmatic and non-magmatic geothermal systems in the Basin and Range province. *Geothermal Resources Council Special Report No. 13*, 93.

Kratt, C., Calvin, W.M., and Coolbaugh, M.F. (2010). Mineral mapping in the Pyramid Lake basin: Hydrothermal alteration, chemical precipitates and geothermal energy potential. *Remote Sensing of Environment 114*, 2297–2304.

Lahsen, A. (1986). Geoquímica de áreas geotermales de la cordillera de los Andes del sur de Chile, entre los 39ºS y 40ºS. *Comunicaciones* , 9-20.

Lahsen, A., Muñoz, N., and Parada, M. (2010). Geothermal Development in Chile. *Proceedings World Geothermal Congress.* Bali, Indonesia.

Lopez, L., and Munizaga, F. (1983). Caracteristicas geoquímicas y Petrogénesis del Complejo Volcánico Laguna del Maule, Andes del Sur, 36º00`S. *Revista Geológica de Chile 10 (2)*, 3-24.

Naranjo, J., and Haller, M. (2002). Erupciones holocenas principalmente explosivas del volcán Planchón, Andes del sur (35°15'S). *Revista geológica de Chile 29*, 93-113.

Noorollahi, Y., Itoi, R., Fujii, H., and Tanaka, T. (2007). GIS model for geothermal resource exploration in Akita and Iwate prefectures, northern Japan. *Computers & Geosciences 33*, 1008–1021.

Sanyal, S.K., Henneberger, R.C., Klein, C.W., and Decker, R.W. (2002). A methodology for Assessment of geothermal Energy Reserves Associated with Volcanic Systems. *Geothermal Resources Council Transactions, Vol. 26* , 22-25.

Sellés, D., Rodríguez, C., Dungan, M.A., Naranjo, J.A., and Gardeweg, M. (2004). Geochemistry of Nevado de Longaví Volcano (36.2°S): geology and geochemistry of a compositionally atypical arc volcano in the Southern Volcanic Zone of the Andes. *Revista geológica de Chile 31*, 293-315.

Smith, R.L., and Shaw, H.R. (1975). Igneous-Related Geothermal Systems. In D.E. White and D.L Williams (eds.), *Assessment of Geothermal Resources of the United States – 1975* (pp. 58-83). Arlington: U.S. Government Printing Office.

Stern, C.R. (2004). Active Andean volcanism: its geologic and tectonic setting. *Revista geológica de Chile 31,* 161-206.

Williams, C.F., Reed, M.J., & Mariner, R.H. (2008). *A Review of Methods Applied by the U.S. Geological Survey in the Assessment of Identified Geothermal Resources.* USGS Open-File Report 2008–1296.